Electronic Supplementary Material (ESI) for Lab on a Chip.

Supporting Information

A droplet microfluidic system for sequential generation of lipid bilayers and transmembrane electrical recordings

Magdalena A. Czekalska[a], Tomasz S. Kaminski[a], Slawomir Jakiela[a], K. Tanuj Sapra[b], Hagan Bayley[b]* and Piotr Garstecki[a]*

[a] *Institute of Physical Chemistry, Polish Academy of Sciences*
Kasprzaka 44/52, 01-224 Warsaw, Poland
E-mail: garst@ichf.edu.pl
[b] *Chemical Biology Sub-Department, University of Oxford, Chemistry Research Laboratory*
12 Mansfield Road, Oxford OX1 3TA, United Kingdom
E-mail: hagan.bayley@chem.ox.ac.uk

Geometry of the chip

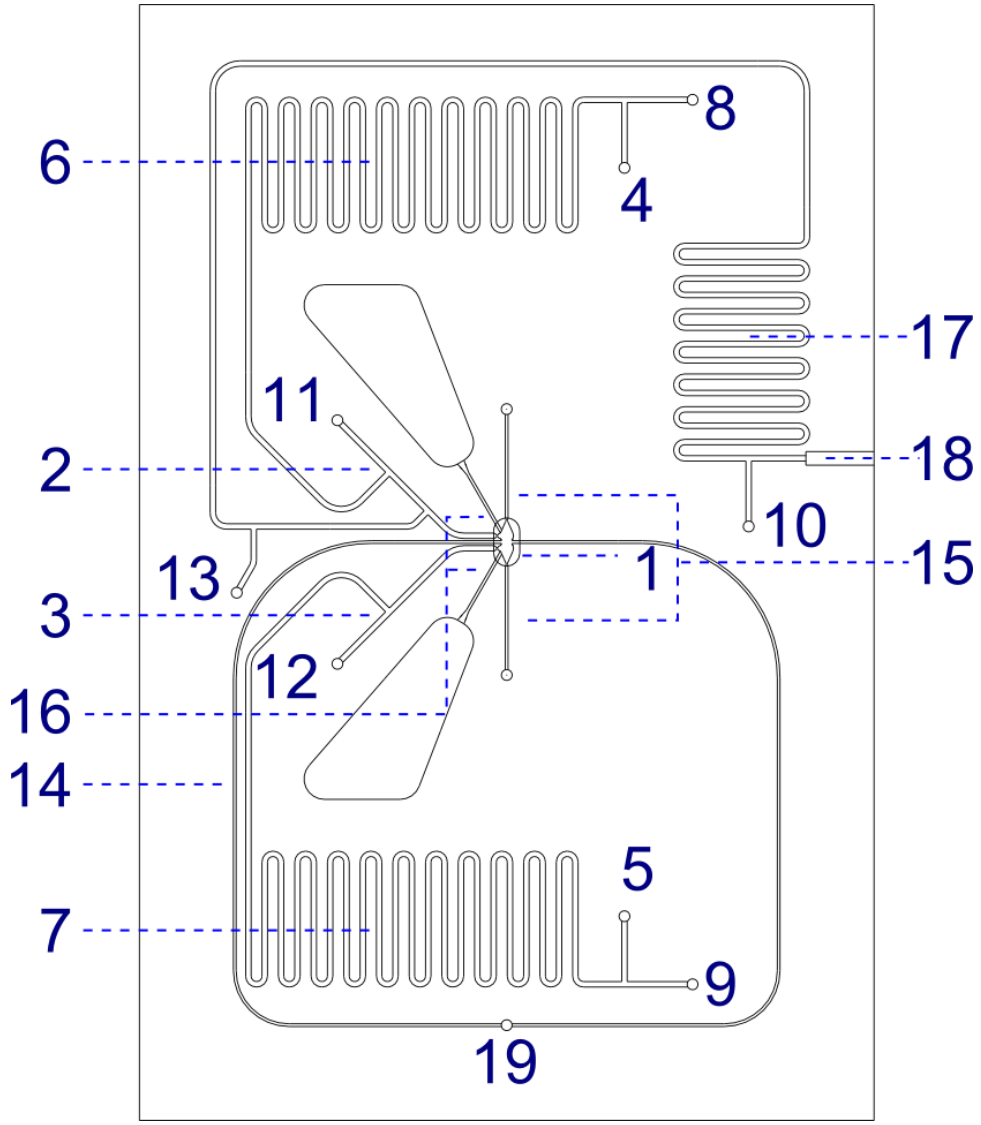

Figure S1. Detailed diagram of the layout of the microfluidic chip. The numbers indicate: 1 - hydrodynamic trap, 2 - T-junction for generation of droplets with buffer, 3 – T-junction for generation of droplets with protein solution, 4 – inlet for the buffer, 5 – inlet for the protein solution, 6 - channels used as a container for buffer, 7 – channels used as a container for the protein solution, 8, 9, 10, 11, 12, 13, 19 – inlets for oil, 14 – channel which supplies oil for the detachment of droplets, 15 – outlet channels, 16 - channels for the pair of electrodes, 17 – channels used as a container for the sequence of inhibitors, 18 – inlet for the tubing containing a sequence of droplets with various concentrations of inhibitor. The dimensions of a whole chip are 82 x 53 mm.

A

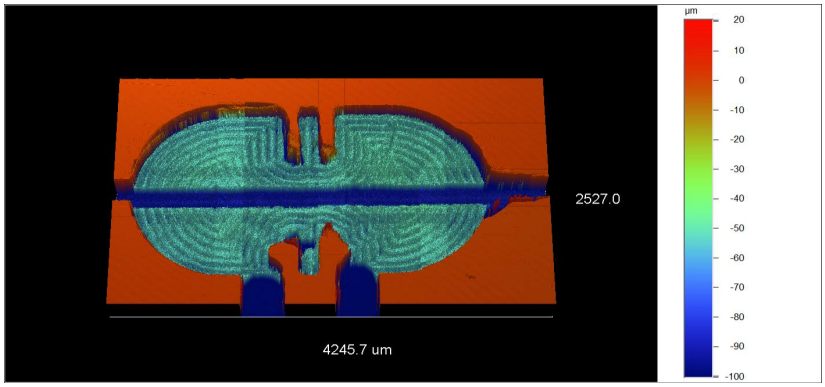

B

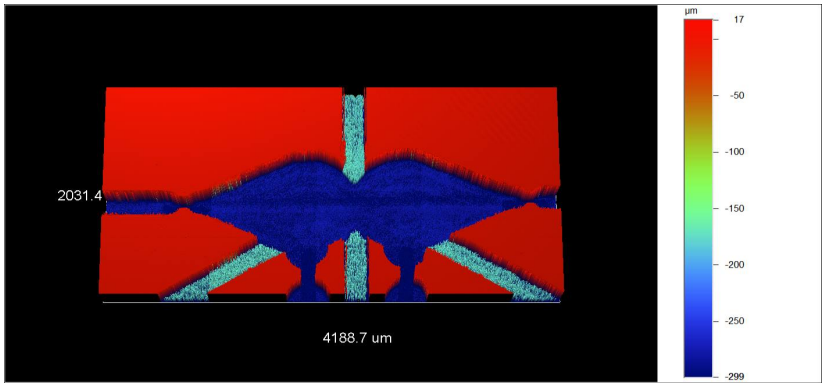

Figure S2. Profilometric scans (Brücker ContourGT-K) depicting the architecture of the microfluidic trap. Parts of the trap were milled in two polycarbonate plates. Upper plate (A) comprises the bypasses and parts of main channels and chamber of the trap. The auxiliary channels for electrodes, perpendicular channels for separation of droplets and other part of the chamber were milled in the lower plate (B).

Description of the experimental system

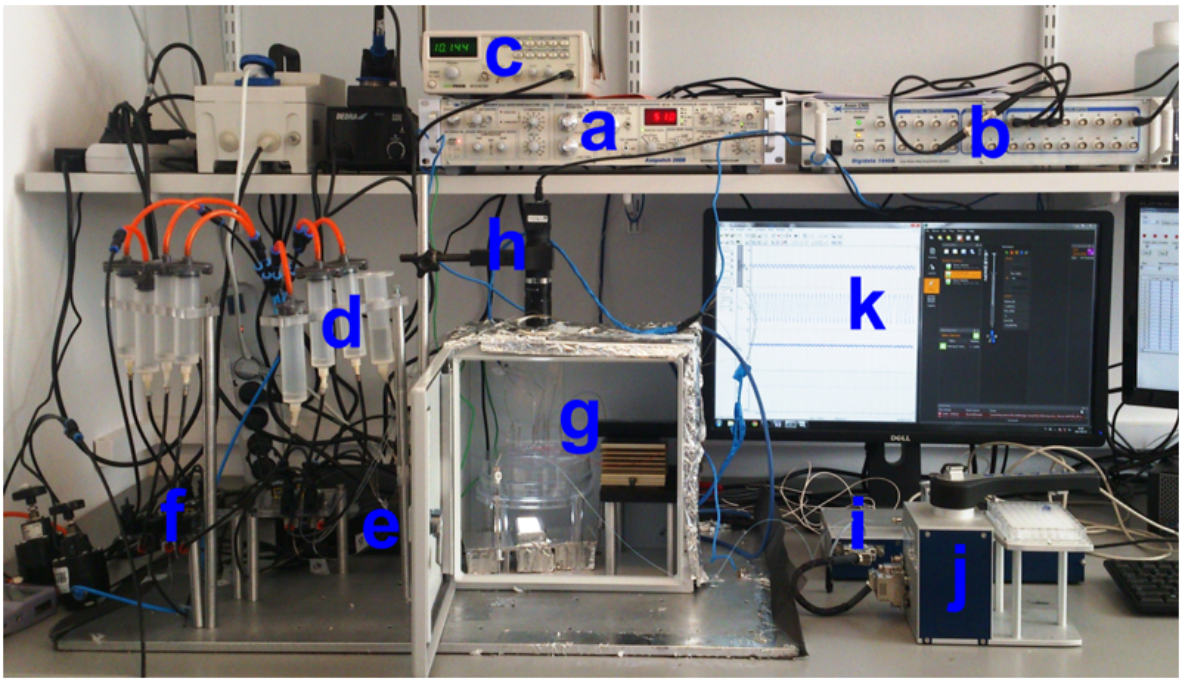

Figure S3. The system for formation of lipid bilayers and electrophysiological measurements consists of several elements:

a. Axon Axopatch 200B Capacitor Feedback Patch Clamp Amplifier (Molecular Devices)
b. Axon Digidata 1440A Digitizer (Molecular Devices)
c. Function generator GFG8216A (ISO-TECH)
d. Oil containers are pressurized by an outer compressor using a manual pressure regulator
e. Electronic valve driver, which is controlled by a NI PCIE-6321 card on a PC. Their construction enables users to generate rectangular pulses, which control the bi-stable coils (Z070D, Sirai). The high state of pulses corresponds to an open valve, while the low state represents a closed valve
f. A set of valves enables us to turn on/off the flow in appropriate channels.
g. Faraday cage AE1033 (Rittal)
h. uEye camera (IDS)

i. Syringe pump neMESYS (Cetoni)

j. Positioning system Rotaxys (Cetoni)

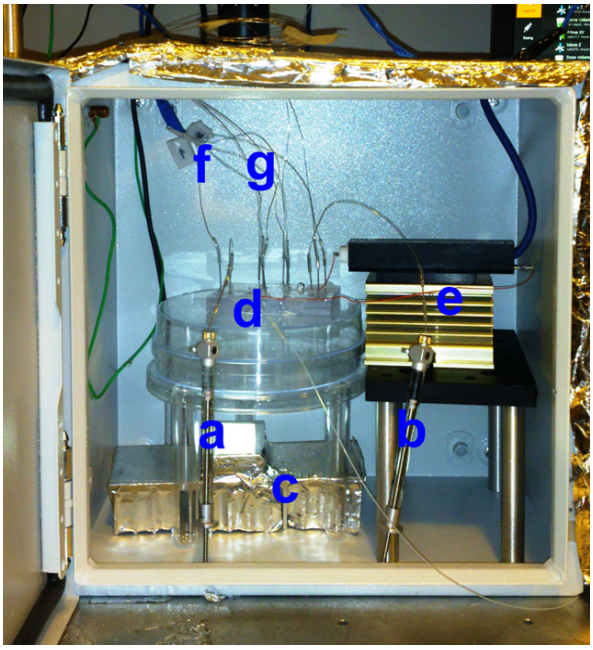

Figure S4. The interior of Faraday cage housing:

a. A syringe filled with buffer

b. A syringe filled with protein solution

c. A source of white light OF-SMD5060NW-H (OptoFlash)

d. The chip positioned on a custom-made transparent platform

e. Headstage with electrodes, placed on a radiator

Operation of the chip

7 valves (V165, equipped with Z070D coils, Sirai, Italy) were controlled with a custom-written Lab View script via a National Instruments (USA) card (NI PCIE-6321). The valves controlled the flow of oil (75% v/v *n*-hexadecane [Alfa Aesar], 25% v/v Ar20 [Sigma Aldrich]) containing 1 mg mL^{-1} of DPhPC (Avanti Polar Lipids) from pressurized reservoirs, through the valves and into the steel capillaries and onto the chip. Setting up the experiment requires a considerable volume of the oil (on the order of few mL). Although the cost of lipids is not high (ca. 1 USD per mL at the concentration that we used), the volume of oil can be minimized to a few hundred microliters. The amount of oil used per exchange of the droplets is very small – below 5 µL.

The aqueous samples (protein solution and buffer) were deposited into long storage channels on the chip directly from syringes, which were closed with valves after the deposition of the sample. Once the liquids were deposited onto the chip, the flow of oil pushed the samples into the on-chip microdroplet generators – T-junctions. We controlled the pressure applied to the

oil reservoirs using manual pressure regulators (Bosch Rexroth PR1-RGP) and monitored the pressure using digital manometers (AZ 82100, AZ Instruments). A reservoir, which supplied the oil to channel no. 14 (see Figure S1), had a separate pressure regulator. We used 10 cm-long HPLC PEEK tubing in order to extend the steel capillary connecting the inlet of this auxiliary channel with the valve. As a result, the resistance of the flow in channel no. 14 was much greater than for the other inlets. In this way, the reduced fluctuations of oil facilitated the process of separation of droplets during their automated exchange in screening experiments.

During the experiments of controlled separation of droplets we used a syringe pump (Nemesys, Cetoni) in order to apply a flow of oil at a defined rate through the channel no. 14.

Efficiency of washing of the electrodes

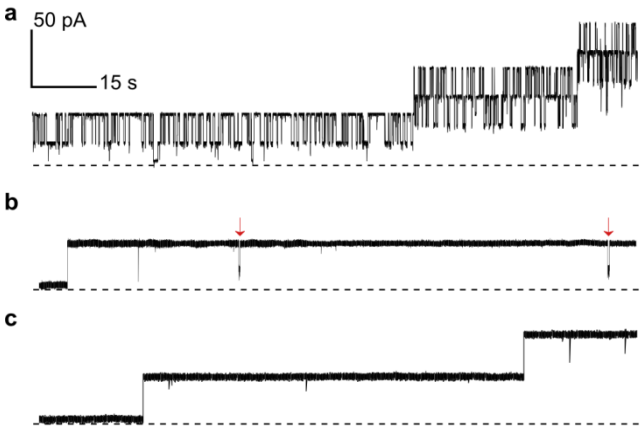

Figure S5. Electrophysiological measurements showing the blocking events and the efficiency of washing the protein inhibitor *γ*-cyclodextrin off the electrode. a) Pore blocking with 50 µM *γ*-cyclodextrin was recorded for 10 minutes. b) The droplet containing the inhibitor was removed from the trap with a stream of oil and replaced with a droplet of pure buffer (1 M KCl, 10 mM Tris-HCl, pH 7.0). A small number of blockades (indicated with red arrows) were recorded. c) After the next droplet of pure buffer was introduced into the trap, no further blockades were observed.

Generation of sequence of droplets containing inhibitors

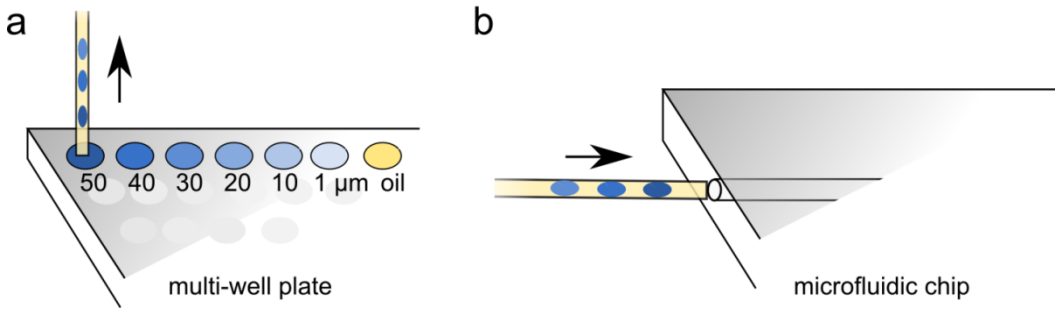

Figure S6. a) A sequence of droplets containing inhibitors was prepared by using a precise syringe pump (Nemesys, Cetoni). Droplets were formed inside PTFE tubing (I.D. 0.3 mm, O.D. 0.6 mm, Bola Bohlender) by alternating aspiration of portions of aqueous samples (300 nL) and oil (700 nL) from a standard 96-well plate. b) The sequence of droplets containing various concentrations of inhibitors was stored inside the tubing and introduced onto the chip by applying the flow from a syringe.

Screening experiment

During the screening experiment the routing of droplets on chip was automated. Prior to the testing of various concentrations of γ-cyclodextrin, we introduced a sequence of inhibitors onto the chip and deposited them in a storage channel. A solution of α-hemolysin was introduced onto the chip from a syringe and a droplet of ~300 nL was generated and locked in a trap on an electrode. Then, we performed the screening experiment according to the following protocol:

Step 1. **Introduction of droplet with inhibitor into the trap:** the precise positioning of a droplet containing inhibitor was aided with an edge-detection algorithm. We used a camera operated on-line by an image processing software that controlled the valves depending on the detected image. The edge of the droplet before entering the trap and then inside of the trap was detected. This was correlated with the opening and closing of appropriate valves.[1]

Step 2. **Formation of bilayer and voltage-clamp measurement (in total 180 s):** in this step the protein was incorporated into the bilayer and inhibitor binding measured.

Step 3. **Removal of droplet with inhibitor and washing of the electrode:** the droplets were separated by the short (1 s) application of the flow of oil through the auxiliary channel no. 14 . Then, a droplet of pure buffer of ~350 nL was generated. The electrode was flushed with the wash droplet, which was not stopped in a trap, however its appearance was detected with edge-detection optical feedback. The script was not continued unless a droplet passed through the trap.

The 3 steps were repeated 12 times, giving 2 full experiments in which 6 concentrations of inhibitor were screened. Next, we introduced a fresh solution of protein.

The voltage of + 50 mV was constantly applied.

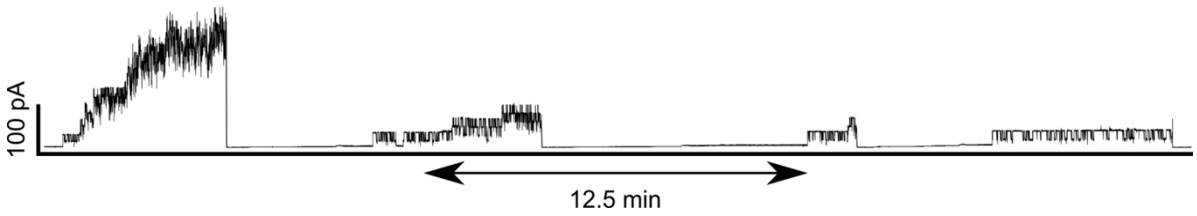

Figure S7. Rapid screening of inhibitors against single α–hemolysin pores. Continuous trace of current shows subsequent incorporation of αHL pores in bilayers formed between a droplet containing a protein solution and 4 successive droplets with decreasing concentrations of γ-cyclodextrin (50, 40, 30 and 20 μM).

Estimation of the Bilayer Size

To estimate the bilayer size, we carried out measurements of capacitive current for pairs of droplets of different volumes (in the range of 250-350 nL). Droplets were generated by aspiring the buffer from a 96-well plate with the aid of a precise pump (Nemesys, Cetoni) and a positioning system (Rotaxys, Cetoni). For each volume we analyzed 5 pairs of droplets. For each pair a triangular potential (10 Hz, 50 mV peak-to-peak) was applied and the resulting square-wave current was recorded at a 1 kHz sampling rate. A model cell with a known capacitance of 100 pF (MCB-1U, Molecular Devices) was used to determine dV/dt (= 1). We collected and analyzed traces of about 60 s. We calculated the average level and standard

deviation of the capacitance (table S1). By using the specific capacitance of a DPhPC bilayer formed in pure hexadecane 0.64 μF cm^{-2},[2] we estimated the contact area between the droplets. We distinguish two sources of variation – one refers to time dependent fluctuations in the area of an individual bilayer, caused by flows and convection in both phases. There is also variation between pairs of droplets, which may be the result of different positioning of each pair of droplets in the trap and variation of droplet volume. The relative standard deviation (RSD) for the bilayer area is in the range of ~5-10% in the case of smaller volumes (250 and 275 nL) and less than 5% for larger droplets. Smaller droplets, even if not positioned exactly in space by the confinement provided by the traps, are attracted to each other during the formation of a bilayer. Nonetheless, the position of smaller droplets in the trap is constrained to a lesser extent than for largest drops.

Table S1. Results of measurements of capacitance and calculations of sizes of bilayers formed between droplets of various volumes.

Droplet no	Droplet volume [nL]	Mean capacitance for a single bilayer [pF]	SD of capacitance for a single bilayer [pF]	Mean capacitance for a volume [pF]	RSD of capacitance for a given volume [pF]	Bilayer area [μm²]
1		152	9			
2		161	5			
3	250,00	165	8	171	10,4%	26 700 ± 2 800
4		176	8			
5		199	5			
6		302	9			
7		331	19			
8	275,00	295	16	308	7,0%	48 200 ± 3 400
9		292	17			
10		323	13			
11		374	8			
12		395	11			
13	300,00	397	19	394	4,1%	61 500 ± 2 500
14		411	7			
15		391	4			
16		521	26			
17		514	16			
18	325,00	546	9	525	4,1%	82 000 ± 3 400
19		534	13			
20		512	19			
21		626	21			
22		618	13			
23	350,00	634	14	627	3,9%	98 000 ± 3 800
24		601	6			
25		658	17			

Calculations of K_d

We analyzed only those fragments of traces that reflected the activity of single αHL pores.

(i) We derived the rate constants from at least three different experiments from single channel recordings with an entire duration of at least 120 s (see table S2).

(ii) We derived the dissociation rate constants, k_{off}, at each concentration as the inverse of the mean residence time (τ_{off}) of γCD within the pore.

(iii) We obtained the association rate constants, k_{on}, from the slope of a plot of the inverse of the mean inter-event interval (τ_{on}) versus the concentration of γCD. Single-channel

recordings have different durations for each experiment so we calculated weighted mean K_d values and weighted mean SDs.

The obtained value of K_d (61 ± 7 μM) is comparable to the value of 47 ± 9 μM, which was calculated by Mantri *et al.*[3] for αHL heptamer at -50 mV (buffer conditions 1M KCl, 25mM Tris HCl and 50 mM EDTA, pH 8). In the aforementioned work the protein was added to the ground electrode compartment. In our set-up the protein is contained within compartment with working electrode. Therefore, due to the phenomenon of rectification of current, we compared our value of K_d (obtained at + 50 mV) to the one obtained at -50 mV.

Table S2. Duration of single-channel recordings in screening experiments.

The table collects times (in seconds) between the insertion of the first and the second nanopore. In some cases, single-channel recording was terminated by exchange of the droplet, according to the described protocol. "x" indicates experiments in which no channel incoroporated into the bilayer.

		Concentration of γ-cyclodextrin [μM]					
		1	**10**	**20**	**30**	**40**	**50**
Screen number	1a	x	93	x	x	24	x
	1b	x	x	57	8	x	x
	2a	x	x	106	24	44	10
	2b	x	x	x	70	x	82
	3a	22	47	x	x	27	16
	3b	x	x	82	x	92	37
	4a	25	x	x	x	66	18
	4b	x	x	20	x	x	x
	5a	62	5	13	15	x	x
	5b	92	x	x	42	34	4
	Total time [s]	**201**	**145**	**278**	**159**	**287**	**167**

Control of the surface area

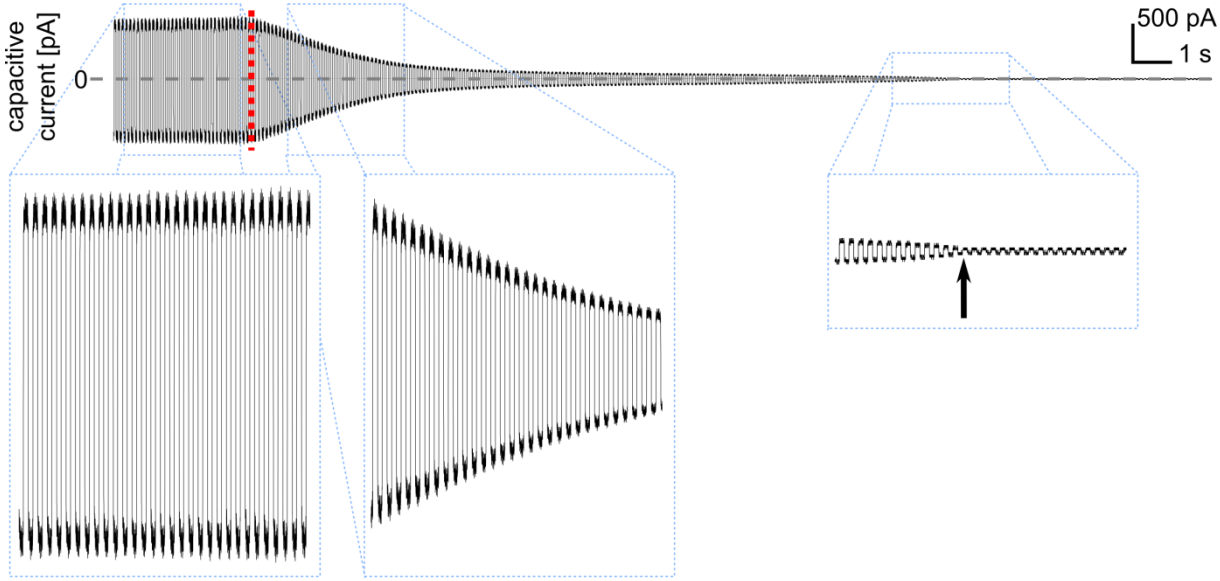

Figure S8. Measurements of capacitive current during separation of droplets. The insets show in detail three different stages of separation. Before the application of oil stream the amplitude of current is steady. The flow of oil from the channel no. 19 (30 nL s^{-1}, beginning of operation indicated with a vertical dotted red line) causes the gradual decrease in bilayer area and in capacitive current. Finally, the droplets become completely separated – this moment is indicated with an arrow.

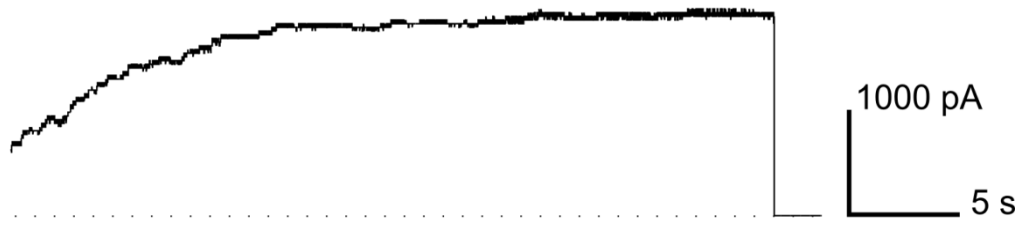

Figure S9. The separation of droplets during the voltage-clamp measurement of *α*HL incorporation. We used a high concentration of protein sample in one of the droplets and observed multiple insertions of pore molecules into the membrane. We applied the flow of oil from the channel no. 19 which resulted in complete separation of droplets, up to the moment of de-attachment. In a voltage-clamp measurement, the separation is seen as a sudden drop of current to the base level.

Image processing

The analysis of electric current traces was performed in Clampfit 10.3. All illustrations were prepared using Inkscape 0.48 software.

References

1 J. Guzowski, P. M. Korczyk, S. Jakiela, P. Garstecki, *Lab. Chip*, 2011, 11, 3593–3595

2 L. C. M. Gross, A. J. Heron, S. C. Baca, M. I. Wallace, *Langmuir*, 2011, 27, 14335–14342.

3 S. Mantri, K. T. Sapra, S. Cheley, T. H. Sharp, H. Bayley, *Nat. Commun*., 2013, 4, 1725.